

# Impact of optical noises on coded Brillouin optical time-domain analyzers

Xia Gao<sup>1</sup>, Zhisheng Yang<sup>2,\*</sup>, Sheng Wang<sup>1</sup>, Xiaobin Hong<sup>1,\*</sup>, Xizi Sun<sup>1</sup>, Jian Wu<sup>1</sup> and Luc Thévenaz<sup>2</sup>

<sup>1</sup>State Key Laboratory of Information Photonics & Optical Communications, Beijing University of Posts and Telecommunications, Beijing 100876, China

<sup>2</sup>EPFL Swiss Federal Institute of Technology, Institute of Electrical Engineering, SCI STI LT, Station 11, CH-1015 Lausanne, Switzerland  
Corresponding author: zhisheng.yang@epfl.ch; xbhong@bupt.edu.cn

**Abstract:** The impact of optical noises on the performance of coded Brillouin optical time-domain analyzers is modelled and experimentally demonstrated. This enables quantitatively evaluating the actual coding gain at any point along the sensing fiber. © 2021 The Author(s)

## 1. Introduction

Distributed optical fiber sensors based on Brillouin optical time-domain analysis (BOTDA) have attracted considerable attentions in recent years, owing to its capability to inform on the spatial distribution of targeted quantities along a long optical fiber (> 25 km) [1]. In BOTDA, the most critical parameter is the measurement signal-to-noise ratio (SNR), which scales and trades-off all critical sensing specifications, such as sensing range, spatial resolution, measurement time and measured accuracy [2]. With the substantial development over the last decade, the performance of the standard single-pulse BOTDA has been optimized towards its physical limits. As an upgrade to the standard BOTDA, optical pulse coding can efficiently increase the SNR with moderate hardware overhead and similar measurement time [1,3]. Ideally, coding techniques operate by launching one or several trains of pulses into the sensing fiber, thus enhancing the signal energy without affecting the detection noise; then, by demodulating (decoding) the backscattered multi-pulse response (coded response) through post-processing, the targeted signal can be retrieved with a reduced noise level. Therefore, the SNR improvement (so-called coding gain) provided by coding techniques is indeed the ratio of the noise level before and after decoding, which is mathematically proportional to square-root of the coding length. Note that this theoretical coding gain can be fully realized only if the noise level remains unchanged when launching the coding sequence instead of a single pulse, which generally means that only the photo-detection thermal noise is considered. However, in the coding scenario the largely enhanced pump energy leads to a considerably enhanced optical noises, which may in turn compromise the above mentioned theoretical coding gain. Despite of abundant studies in relation to coding techniques [1,3,4,5], the impact of optical noises on the coding gain has not yet been clearly documented. This hinders a full evaluation on the performance of coding techniques under a given experimental condition.

In this paper, noises impacting on the performance of coded DOTDA are theoretically modeled and experimentally verified for both Brillouin loss configuration (BLC) and Brillouin gain configuration (BGC). It turns out that optical noises, including the polarization noise and spontaneous Brillouin scattering (SpBS) to signal beating noise, may be largely enhanced by the use of optical coding sequence compared to those in the single pulse scheme. At the beginning of the sensing fiber, these optical noises are far larger than the photo-detection thermal noise, so that the theoretical coding gain is largely compromised. Along the sensing fiber, the contribution of optical noises reduces due to the fiber attenuation, whilst the thermal noise remains unchanged; in this case the penalty on the coding gain due to optical noise is reduced, depending on the examined fiber position.

## 2. Principle

The analysis is here performed based on a standard setup for unipolar coded BOTDA [4], in which a polarization scrambler is employed to mitigate the impact of polarization pulling effects. The noise model is established by assuming that the BFS profile is uniform, corresponding to the worst case, i.e., the negative impact of the additional Brillouin-gain dependent noises is the most detrimental. Considering both the optical noise and detector noise, for the  $n^{th}$  single acquisition (i.e. non-averaged), the photocurrent of the detected optical signal (raw coded BOTDA trace) at the Brillouin resonance can be expressed as [4]:

$$I_c(t, n) = \eta P_S^{DC} \exp[G(t, n)] + e_{SpBS}(t, n) + e_{PD}(t, n) \quad (1)$$

where  $t$  stands for the sampling time,  $\eta \approx 1$  A/W is the responsivity of the photodetector,  $P_S^{DC}$  is the power of the DC-probe reaching the receiver,  $e_{SpBS}(t, n)$  and  $e_{PD}(t, n)$  denote the SpBS-probe beating current noise and photo-

detection current noise, respectively.  $G(t, n)$  represents the cumulated linear Brillouin gain at the Brillouin resonance provided by all pulses in the coding sequence, which can be expressed as:

$$G(t, n) = K \sum_{i=1}^{L_C} g_B(t) C_i \cos^2 \theta(i, t, n) \quad (2)$$

where  $g_B(t)$  is the single-pulse Brillouin gain at the Brillouin resonance,  $L_C$  and  $C_i$  denote the code bit number and the state (either 0 or 1) of the  $i^{th}$  coded pulse, respectively;  $K$  is a scaling factor that accounts for the longitudinal rotations of the local polarization principle axis, obtained by calculating the square root of the ratio between the average variance and maximum variance of a single-pulse Brillouin gain trace, leading to  $K = 0.67$  according to experimental results;  $\theta(i, t, n)$  is the relative polarization angle between the  $i^{th}$  coded pulse and the probe wave, which is randomly distributed over the interval  $[0, \pi]$ . Note that for a given sampling time  $t$ , the polarization angle  $\theta$  varies as a function of acquisition number  $n$  due to the use of the polarization scrambler. This polarization-induced variation, here referred as the polarization noise, can be characterized by its standard deviation expressed as:

$$\sigma_{pol}(t) = K \sqrt{\langle G(t, n)^2 \rangle_n - \langle G(t, n) \rangle_n^2} = \frac{KG(t)}{\sqrt{2M}} = \frac{K\sqrt{g_B(t)G(t)}}{2} \quad (3)$$

where  $G(t)$  is the mean accumulated linear Brillouin gain at the Brillouin resonance, which does not suffer from polarization noise. Mathematically,  $G(t) = \langle G(t, n) \rangle_n = Mg_B(t)/2$ , where  $M$  is the number of '1' elements in the coded pulse.

After applying the logarithmic normalization on the Eq. (1) (to ensure a distortion-free decoding [4]), the retrieved signal that will be used for decoding can be expressed as:

$$G_{linear}(t, n) = \ln \left[ \frac{I_C(t, n)}{\eta P_S^{DC}} \right] \approx G(t, n) + \frac{e_{SpBS}(t, n)}{P_S^{DC} \exp[G(t, n)]} + \frac{e_{PD}(t, n)}{P_S^{DC} \exp[G(t, n)]} \quad (4)$$

whose repeatability is affected by 3 noise sources present in the three terms, respectively:

- 1) *polarization noise* (presented in the first term of Eq. (4)), whose standard deviation is described by Eq. (3).
- 2) *Signal-SpBS beating noise* (presented in the second term of Eq. (4)), which comes from the beating between the SpBS originated from the coded pulse sequence ( $E_{SpBS}$ ) and the probe signal ( $E_S$ ) reaching the photodetector. The noise STD can be calculated as:

$$\sigma_{SpBS-S}(t) = \sqrt{\frac{E_{SpBS}^2(t) E_S^2(t)}{P_S^{DC} \exp[G(t)]}} = \sqrt{\frac{P_{SpBS}^C(t)}{P_S^{DC} \exp[G(t)]}} \propto \sqrt{\frac{G(t)}{P_S^{DC} \exp[G(t)]}} \quad (5)$$

where  $P_{SpBS}^C(t) = M\alpha_{SpBS}\Delta z P_p(t)$  representing the power of SpBS originated from the coding sequence;  $\alpha_{SpBS}$ ,  $\Delta z$  and  $P_p(t)$  are the scattering coefficient of SpBS, spatial resolution and pulse power, respectively. Notice that  $M\Delta z P_p(t)$  represents the energy of coded pulse, which is proportional to the mean accumulated Brillouin gain  $G(t)$ , while  $\alpha_{SpBS}$  is a constant for a given sensing fiber. This means  $P_{SpBS}^C(t)$  is proportional to  $G(t)$ , as  $P_{SpBS}^C(t) \propto G(t)$ .

- 3) *Photo-detection noise* (presented in the third term of Eq. (4)), attributed to thermal noise and shot noise. However, due to the low optical probe power reaching the receiver, the shot noise contribution can usually be ignored. Thus, the noise STD is only related to the thermal noise and can be expressed as:

$$\sigma_{PD}(t) \approx \frac{\sqrt{\sigma_{th}^2}}{P_S^{DC} \exp[G(t)]} \quad (6)$$

where  $\sigma_{th}^2$  is the thermal noise variance, which can be readily characterized by measuring the photodetector output without input light [6].

Practically, for any spatial resolution that corresponds to a specific optimized single pulse gain  $g_B(t)$ , both the optimized mean accumulated Brillouin gain  $G(t)$  and the power of the DC-probe  $P_S^{DC}$  reaching the receiver are fixed for a given experimental condition. The former is limited by undesired physical phenomena in the optical fiber (e.g. high-order pump depletion [4]), the latter should be close to the saturation power of the used photo detector for a highest possible SNR. In this case, the polarization noise expressed by Eq. (3) is only positively related to the corresponding  $g_B(t)$  (determined by the used spatial resolution), while both the SpBS-signal beating noise and thermal noise, expressed by Eq. (5) and (6) respectively, remain fixed. Fig. 1 (a) and (b) illustrates the theoretically

calculated STD of above addressed noises based on Eq. (3), (5) and (6), as a function of  $g_{B0}$  that represents the single-pulse Brillouin gain at the fiber start end, for Brillouin gain configuration (BGC) and Brillouin loss configuration (BLC), respectively. In the calculation,  $P_S^{DC}$  is set to -20 dBm to match the practical saturation power of the photo receiver that will be used in the experiment, and  $G_0$  (denotes the accumulated Brillouin gain near the fiber start end) is set to 100% that is a safe level avoiding possible decoding distortion [4]. From Fig. 1, it can be clearly seen that, as the  $g_{B0}$  increases (corresponding to the increase of spatial resolution), the polarization noise increases and gradually dominates. On the contrary, the thermal noise and SpBS-signal beating noise remain constant, and the latter is constantly larger than the former. Note that these two noises levels for BLC are slightly larger than those for BGC, which is caused by the opposite signs in front of the term  $G(t)$  in Eq. (5) and (6). Figures clearly show that the optical noises (polarization noise and SpBS-signal beating noise) dominate the total noise at the fiber start end, for any spatial resolution; this practically compromises the theoretically calculated coding gain ( $\sqrt{L_c}/2$ , where  $L_c \approx 2G(t)/g'_B(t)$  denotes the code length,  $g'_B(t) = g_B(t)/2$  representing the mean single-pulse gain at the Brillouin resonance) that only considers the thermal noise. However, due to the fiber loss, these optical noises decays as a function of distance (i.e., variable  $t$  in equations), while the thermal noise attributed to the photo receiver remains unchanged. Therefore, the optical noises may negligibly contribute (i.e. the theoretical coding gain might be reached) at the fiber far-end, depending on the fiber length.

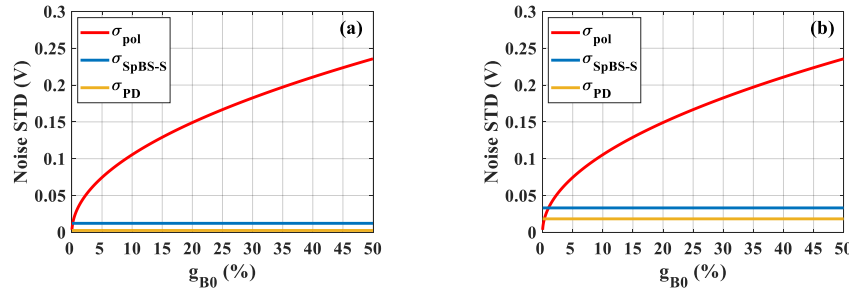


Fig.1 STD of noises as a function of  $g_{B0}$  for (a) BGC and (b) BLC. Simulation's parameters are:  $G_0 = 100\%$ ;  $K = 0.67$ ;  $P_S^{DC} = -20\text{ dBm}$ ;  $P_p = +20\text{ dbm}$ ;  $\alpha_{SpBS} = -93\text{ dBm}/(\text{m} \cdot \text{mW})$ ;  $\sigma_{th} = 0.0094\text{ V}$ .

### 3. Experimental results and discussion

Experiments based on the typical coded-BOTDA setup [4] are carried out to demonstrate the theoretical noise characterizations, and to investigate how the optical noises impact on the coding gain as a function of fiber distance. In our study, flat Simplex code sequences are employed for all experiments. At the receiver part, the bandwidth and saturated power of PD are 75 MHz and -18 dBm, respectively. A 50 km-long SMF is used, which is connected by two ~25 km fiber spools with similar BFS.

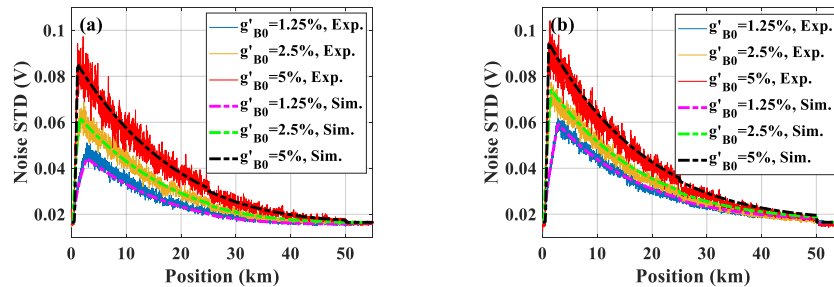


Fig.2 STD of 20 consecutive noises obtained without average over 50 km fiber for different single-pulse Brillouin gain for (a) BGC and (b) BLC. Dash-dot lines are the simulation curves of corresponding noise.

Comparisons with different mean single-pulse Brillouin gain, i.e.,  $g'_{B0} = \sim 5\%$ ,  $\sim 2.5\%$  and  $1.25\%$ , respectively, are performed for both BGC and BLC. In all cases, the optical power of the DC-probe is set to -24 dBm, and the mean accumulated Brillouin gain  $G_0$  is fixed as  $\sim 75\%$ , corresponding to the coding length  $L_c$  of 31 bits, 63 bits and 127 bits, respectively. The noise STD profile as a function of distance in each case is computed from 20 consecutive measurements with no trace average, as shown in Fig. 2(a) and (b), for BGC and BLC, respectively. Theoretical profiles predicted by equations in previous section are also plotted as dashed curves, being in good agreement with measurements.

Then, the impact of the characterized noises on the coding gain is experimentally investigated, with optimized BGC and BLC. Firstly, reference measurement is performed using an optimized single-pulse scheme, with a spatial

resolution of 2 m, corresponding to an optimized mean single-pulse Brillouin gain  $g'_{B0}$  of 2.5%. The probe power is set to  $-20$  dBm that is close to the PD saturation power. On the other hand, in optimized coded-BOTDA schemes, the power of each coded pulse is adjusted equal to that of the optimized single pulse. A 63-bit Simplex code is employed, providing a mean accumulated Brillouin gain  $G_0 \approx 75\%$ . The power of the DC-probe reaching the receiver is set to  $-20$  dBm (equal to that of single-pulse scheme) for BLC, and set to  $-24$  dBm for BGC to prevent PD from saturated by the Brillouin-amplified probe signal. The STD of noises for the 3 above-mentioned conditions, as well as the theoretical predictions, are shown in Fig. 3(a), all obtained without average. Notice that, at the fiber input, coding sequence introduces  $\sim 4.25$  times higher noises than that of the optimized single-pulse case, which would greatly compromise the code gain. Due to the fiber attenuation, optical noises gradually reduce, resulting in  $\sim 1.02$  and  $\sim 1.25$  times higher noises near the far-end of 50 km fiber, for BGC and BLC, respectively. Although the impact of optical noise at the fiber far-end is largely reduced compared to that at the fiber near-end, it would still lead to a non-negligible penalty on the coding gain. This can be quantified by comparing the SNR profile after decoding, as shown in Fig. 3(b), where all traces are averaged by 1024 times for the sake of visual clarity. It can be found that in the case of BLC (black curve), the SNR improvement compared to the single pulse case at the fiber far-end is 5 dB, being 1 dB lower than the theoretical coding gain of 6 dB ( $= 10\lg(\sqrt{63}/2)$ ). The SNR improvement in the case of BGC (red curve) is even lower, due to the lower probe power used. At last, the BFS profile along the fiber is estimated using the cross-correlation method [7] for all three cases, and the corresponding BFS uncertainty profiles are shown in Fig. 3(c). Behaviors match well with Fig. 3(b), fully demonstrating the negative impact of the optical noise on the coding gain.

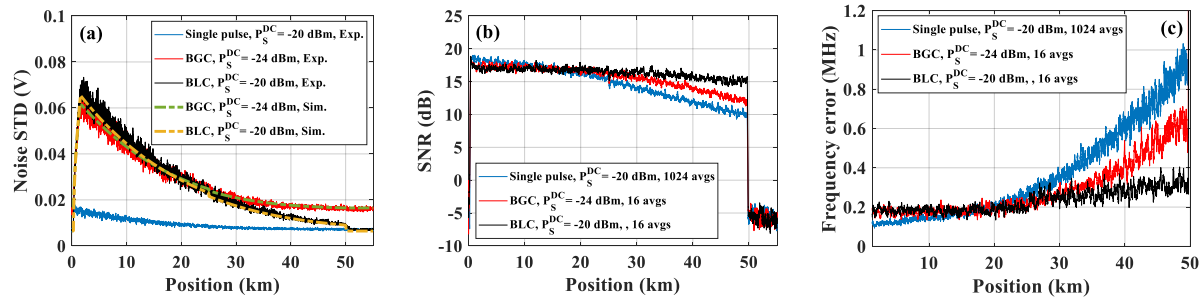


Fig. 3 (a) STD of noises obtained by 20 consecutive measurements without average, over 50km fiber, for optimized single-pulse system and 63 bits coded system, where dash-dot lines are the simulation curves of corresponding noises; (b) SNR profiles at the Brillouin resonance; (c) BFS uncertainty profiles along the 50km fiber.

#### 4. Conclusion

In conclusion, the noise model for coded-BOTDA has been theoretically established and experimentally validated for the first time. Results point out that the noise sources in coded-BOTDA mainly contain the polarization noise, SpBS-signal beating noise and the photo-detection thermal noise. In particular, the level of optical noises is positively related to the accumulated Brillouin gain, while the thermal noise remains constant. The model allows for evaluating the actual coding gain at any fiber position for any given experimental scenario. It turns out that, at the near end of sensing fiber where the accumulated Brillouin gain is generally high, the coding gain is largely deteriorated from the theoretical value. At the fiber far-end, the local Brillouin gain reduces due to the fiber attenuation, so that the penalty of coding gain due to optical noises is alleviated accordingly. It should be noted that the theoretical coding gain may never be reached (i.e. the optical noises may never be fully neglected), depending on the fiber length.

**Acknowledgement:** National Natural Science Foundation of China under Grant 61875018.

#### 5. References

- [1] A. H. Hartog, *An Introduction to Distributed Optical Fiber Sensors* (Boca Raton, 2017).
- [2] M. A. Soto and L. Thévenaz, "Modeling and evaluating the performance of Brillouin distributed optical fiber sensors," Opt. Express **21**, 31347–31366 (2013).
- [3] M. A. Soto, *Distributed Brillouin Sensing: Time-Domain Techniques* (Singapore, 2018).
- [4] Z. Yang, Z. Li, S. Zaslawski, L. Thévenaz, and M. A. Soto, "Design rules for optimizing unipolar coded Brillouin optical time-domain analyzers," Opt. Express **26**, 16505–16523 (2018).
- [5] Y. Zhou, L. Yan, Z. Li, W. Pan, and B. Luo, "Polarization division multiplexing pulse coding for eliminating the effect of polarization pulling in Golay-coded BOTDA fiber sensor," Opt. Express **26**, 19686–19693 (2018).
- [6] S. Wang, Z. Yang, M. A. Soto, L. Thévenaz, "Optimizing the signal-to-noise ratio for direct-detection BOTDA," Seventh European Workshop on Optical Fibre Sensors, **11199**, 111992C (2019).
- [7] S. M. Haneef, Z. Yang, L. Thévenaz, D. Venkitesh, and B. Srinivasan, "Performance analysis of frequency shift estimation techniques in Brillouin distributed fiber sensors," Opt. Express **26**, 14661–14677 (2018).